

OPEN ACCESS

EDITED BY Benjamin Costas, University of Porto, Portugal

REVIEWED BY
Carlo C. Lazado,
Fisheries and Aquaculture Research (Nofima),
Norway
Yuwen Dong,
University of Pennsylvania, United States

*CORRESPONDENCE
Mariano del Sol

mariano.delsol@ufrontera.cl
Mariana Rojas
mrojasr@u.uchile.cl

RECEIVED 08 August 2025 ACCEPTED 16 October 2025 PUBLISHED 03 November 2025

CITATION

Smok C, Rojas M, Aguila MB and del Sol M (2025) Regenerative responses and structural plasticity of gills in Atlantic salmon. Front. Mar. Sci. 12:1682427. doi: 10.3389/fmars.2025.1682427

COPYRIGHT

© 2025 Smok, Rojas, Aguila and del Sol. This is an open-access article distributed under the terms of the Creative Commons Attribution License (CC BY). The use, distribution or reproduction in other forums is permitted, provided the original author(s) and the copyright owner(s) are credited and that the original publication in this journal is cited, in accordance with accepted academic practice. No use, distribution or reproduction is permitted which does not comply with these terms.

Regenerative responses and structural plasticity of gills in Atlantic salmon

Carolina Smok^{1,2}, Mariana Rojas^{2*}, Marcia B. Aguila³ and Mariano del Sol^{1,4*}

¹Doctoral Program in Morphological Sciences, Universidad de La Frontera, Temuco, Chile, ²Laboratorio de Embriología Comparada, Núcleo Interdisciplinario de Biología y Genética, Instituto de Ciencias Biomédicas (ICBM), Facultad de Medicina, Universidad de Chile, Santiago, Chile, ³Laboratory of Morphometry, Metabolism and Cardiovascular Disease, Institute of Biology, Biomedical Center, The University of the State of Rio de Janeiro, Rio de Janeiro, Brazil, ⁴Center of Excellence in Morphological and Surgical Studies, Universidad de la Frontera, Temuco, Chile

Introduction: Gill regeneration in teleosts represents a key adaptive mechanism for maintaining respiratory efficiency under environmental stress. This study provides the first detailed histological characterization of branchial regeneration in Atlantic salmon (*Salmo salar*) smolts reared under freshwater hatchery conditions.

Material and methods: Fifty clinically healthy smolts were analyzed through anatomical, histological, and microcomputed tomography (micro-CT) approaches.

Results: We observed that the regenerative blastema first gave rise to primary filaments with developing lamellae; subsequently, from this same structure, a second generation of filaments emerged, demonstrating the capacity of the blastema to produce multiple waves of filament outgrowth. Unlike zebrafish, where branchial regeneration after filament resection has been widely described, regeneration in Atlantic salmon occurs more slowly and has been poorly characterized despite its relevance for aquaculture. Quantitative morphometry showed that the blastema occupied 8–19% (mean 14%) of total gill area and correlated positively with the number of regenerated filaments (ρ = 0.5; ρ ≈ 0.011). PCNA immunostaining revealed active cell proliferation within filament cartilage (mean index: 38.9 \pm 13.5%), confirming its role as a substrate for regeneration. Newly formed tissues exhibited differentiation into hyaline cartilage, smooth and striated muscle, and vascular structures. Lamellar density remained lower in regenerating filaments (33.8 \pm 15.9 per 0.5 mm²) compared to healthy ones (48.6 \pm 19.3 per 0.5 mm²; ρ = 0.013), indicating incomplete maturation during smoltification.

Discussion: These findings demonstrate that branchial regeneration in *S. salar* occurs naturally, without amputation, likely as an adaptive response to transient hypoxia. Recognizing these histological patterns allows distinguishing physiological regeneration from pathology and offers new criteria for welfare and smolt-readiness assessment in aquaculture.

KEYWORDS

hypoxia, Salmo salar, micro-computed tomography, branchial arch, aquaculture welfare, gill regeneration, gill health

Introduction

The gills of teleost fish are multifunctional organs that play essential roles in gas exchange, osmoregulation, nitrogen excretion, and immune defense. Their complex anatomical architecture includes branchial arches, filaments, and lamellae, containing a wide diversity of epithelial, connective, and vascular cells. This structural complexity is matched by a remarkable plasticity, which enables gills to respond dynamically to environmental and physiological challenges such as hypoxia, temperature fluctuations, pollutants and infectious agents (Ghanizadeh-Kazerouni et al., 2024; Król et al., 2020; Nilsson et al., 2012; Sundell and Sundh, 2012).

The life cycle of the Atlantic Salmon (Salmo salar) includes multiple differentiated stages, spanning from the moment of egg fertilization until the individual reaching sexual maturity. Each stage is associated with adaptive physiological and morphological changes. In this transformation process, smoltification represents a crucial phase, marked by an accelerated gill growth and the differentiation of specialized cellular types such as ionocytes, which enable tolerance to variations in environmental salinity (Houde et al., 2019; McCormick, 2012; Morera et al., 2021; Robertson and McCormick, 2012).

The gills of teleost fish are constituted by four pairs of branchial arches, each presenting two parallel rows of filaments projecting towards the aquatic environment. In salmonids, those filaments are joined by a cartilaginous septum that extends up to half their length, providing structural support (Ghanizadeh-Kazerouni et al., 2024). Perpendicularly oriented to the filaments, emerge the lamellae, respiratory functional units that maximize the surface dedicated to gas exchange (Pan et al., 2021). Filaments and lamellae are lined by an epithelium that includes squamous, pillar, ionocytes (mitochondria-rich cells), mucosal, immune, undifferentiated, and neuroepithelial cells (Ghanizadeh-Kazerouni et al., 2024; Sales et al., 2017; Stolper et al., 2019).

Teleost gills exhibit continuous growth and regeneration throughout life, allowing restoration even after significant amputations (Mierzwa et al., 2020). and maintaining regenerative capacity across the entire lifespan (Jonz, 2024). This process depends on the formation and maintenance of a vascular niche and an adequate nerve supply. Both requirements are fundamental to support new tissue proliferation, comparable to the mechanisms observed in mammalian lung regeneration (Messerli et al., 2020).

Gill plasticity and remodeling have been described as a response to hypoxia, ammonium exposure, temperature variations, and exercise (Ghanizadeh-Kazerouni et al., 2024). Such branchial remodeling, reversible within hours to days, has been observed in cyprinids, eels, salmonids, anabantids, and killifish (Nilsson, 2007; Sollid et al., 2003). These manifestations of morphological plasticity involve apoptosis, proliferation, and extracellular matrix modifications that safeguard functional integrity while adapting to environmental demands (Ghanizadeh-Kazerouni et al., 2024; Nilsson et al., 2012). Gills thus represent valuable biomarkers of fish welfare and environmental stress (Luzio et al., 2013; Roa et al., 2011; Strzyzewska et al., 2016).

Gill regeneration proceeds through three principal phases: (i) wound healing, (ii) blastema formation, and (iii) tissue reconstruction, involving coordinated blastemal cell proliferation, differentiation, and tissue reorganization. This process has been extensively characterized in zebrafish, where experimental gill filament resection induces blastema-like proliferative zones that generate new filaments and lamellae (Cadiz and Jonz, 2020; Mierzwa et al., 2020; Saito et al., 2019). In salmonids, however, mechanistic understanding remains limited. Pharmacological inhibition of key signaling pathways (FGF, BMP, Notch, Shh) reduces filament growth, underscoring their central role in early regenerative events (Cadiz et al., 2024). Complementarily, singlecell transcriptomic atlases have provided detailed molecular characterization of the gill cellular diversity in zebrafish, identifying oxygen-sensitive neuroepithelial cells that proliferate under hypoxia (Pan et al., 2021).

Proliferating cell nuclear antigen (PCNA) is a conserved marker of cells undergoing DNA replication and has been widely used to evaluate mitotic activity in regenerative processes (Sales et al., 2017; Singh et al., 2025). In fish models, PCNA immunolabeling has revealed proliferative zones in regenerating gill filaments, supporting its use as a reliable biomarker of blastema formation and cellular turnover (Mierzwa et al., 2020).

In salmonids, however, the mechanistic understanding remains limited. Recent studies have focused on applied aspects: development of the Atlantic salmon gill epithelial cell line (ASG-10) for barrier and immunity research (Slattery et al., 2023; Solhaug et al., 2024), and experimental filament resection models demonstrating partial regenerative capacity depending on the magnitude of the injury and the metabolic state (Ghanizadeh-Kazerouni et al., 2024, 2025). In particular, mitochondrial respiratory capacity directly influences regenerative outcomes in Atlantic salmon (Ghanizadeh-Kazerouni et al., 2025). Despite these advances, a comprehensive histological characterization of gill regeneration in Atlantic salmon during critical stages such as smoltification remains lacking, limiting the ability to distinguish adaptive physiological remodeling from pathological lesions in aquaculture systems (Mitchell and Rodger, 2011; Powell et al., 2015).

The present study aims to bridge basic biological insights with aquaculture needs. Unlike zebrafish, who present accelerated development at high temperatures, salmonids develop slowly at low environmental temperatures (~8 °C), where fluctuations can trigger malformations. Moreover, Atlantic salmon undergo smoltification, a unique transition from freshwater to seawater, which is absent in zebrafish (Morera et al., 2021; Stefansson et al., 2012). Misinterpretations of regenerative versus pathological changes may lead to unnecessary culling of fish. Therefore, this study emphasizes the applied dimension of gill regeneration research, providing histological criteria to guide aquaculture health monitoring.

Several scoring systems have been developed to evaluate gill health, ranging from macroscopic 0–5 scales to histopathological approaches that emphasize lesions such as lamellar hyperplasia, necrosis, edema, and pathogen presence (Costelloe et al., 2025;

Fridman et al., 2021; Gjessing et al., 2019; Mitchell et al., 2012). However, these systems are mainly focused on infectious conditions, whereas environmental stressors such as hypoxia or temperature fluctuations (Ghanizadeh-Kazerouni et al., 2024) may elicit comparable biological mechanisms, including cell proliferation and differentiation, often accompanied by regenerative remodeling and plastic adaptations such as filament calcification (Smok et al., 2025a).

Unlike *Danio rerio*, salmonids exhibit a slow branchial ontogeny, with lamellae still incomplete before three weeks post-hatching (Peñailllo, 2011). In some pre-smolt and smolt salmon, a reparative blastema may appear, associated with the regeneration of filaments and lamellae. This process differs markedly from that described in laboratory model species, making this knowledge particularly novel and relevant (Smok et al., 2025a, 2025b).

Despite these advances, knowledge on gill regeneration in Atlantic salmon (*Salmo salar*) remains fragmentary. Most studies in salmonids focus on morphological outcomes or welfare scoring systems (Mitchell and Rodger, 2011; Powell et al., 2015), while the cellular origins and molecular pathways driving regenerative responses are still poorly understood. A major challenge lies in distinguishing between adaptive remodeling and pathological lesions under intensive aquaculture conditions.

The hypothesis underlying our study is that gill regeneration in Atlantic salmon involves the formation of a proliferative blastema that differentiates into multiple tissue types, providing histological criteria to distinguish adaptive remodeling from pathological alterations. This perspective highlights regeneration as a process that contributes to gill health, with potential implications for diagnostic frameworks and aquaculture practices.

Material and methods

Origin of fish and rearing conditions

The study was conducted at a freshwater hatchery located in Región de Los Lagos, in southern Chile. Fish proceeding from the same lot were monitored since the year 2023 through anatomical and histological analyses at two ontogenetic stages: (1) alevin–parr (May–June) and (2) smolt (September–October). This longitudinal approach allowed the recording of morphological alterations and gill regeneration processes at different developmental stages.

Sampling of the alevin-parr stage was included as part of a previous ontogenetic analysis performed every 3–4 months to evaluate the normality of development. This analysis showed that most individuals presented normal gill morphology, with limited findings such as filament hyperplasia or mild branchial arch alterations, and no blastema formation was evidenced. Therefore, the present study focuses exclusively on the gills obtained during the smolt stage.

Smolt salmon were maintained in a recirculating aquaculture system (RAS). The water was treated by reverse osmosis to control

dissolved minerals and optimize water quality. Environmental parameters during rearing were maintained at dissolved oxygen levels of 80–90% and pH ranging from 6.5 to 7.0. An Oxyguard monitor controlled the culture at a constant temperature of 9 °C and 100% oxygen saturation.

Fifty smolt salmons were selected, externally characterized by their silvery coloration and absence of parr marks. The fish corresponded to the species *Salmo salar* in the initial phase of smoltification (>15 cm total length, 80–120 g body weight, ~2500 accumulated thermal units [ATU] post-hatching), fulfilling the criteria of smoltification described in salmon aquaculture (Khaw et al., 2021; Morera et al., 2021).

Prior to sampling. The fifty specimens were clinically evaluated prior to sampling, considering external welfare indicators such as body weight, skin and scale integrity, opercular morphology, mandibular structure, spinal alignment, fin morphology, and the absence of ectoparasites (*Caligus* sp.) (Suarez et al., 2021). In addition, a histopathological assessment of the gills was conducted (evaluating branchial arch deformation, epithelial hyperplasia, lamellar fusion, filament cartilage deformation, and cartilage calcification) using a standardized scoring system (Bloecher et al., 2024; Clinton et al., 2024). The combination of these evaluations ensured that only clinically healthy fish, free of subclinical pathologies, were included in the present study. Furthermore, only fish fulfilling welfare requirements were included in the study.

No experimental manipulations or injuries were induced. However, under intensive production, transient hypoxia or minor mechanical stress can occur, potentially triggering localized regenerative responses. Thus, the observed blastema and neofilaments likely represent the intrinsic regenerative capacity of gill tissue under real environmental conditions, rather than a pathological or experimentally induced state. However, under intensive RAS conditions, transient hypoxia episodes may occur that, although not affecting the entire population homogeneously, can trigger localized blastema formation in some individuals.

In accordance with ethical regulations for research with experimental animals, the protocol was reviewed and approved by the Faculty Ethics Committee (ACTA No. 14321) of Research Project No. 072/21, Universidad de La Frontera (Temuco, Chile). Fish did not experience pain, stress, or distress. They were euthanized by immersion in an overdose of 5% benzocaine (BZ-20[®], Veterchemical).

Sampling strategy

From the total of 50 smolts evaluated, 28 fish were processed for histology and morphological assessment. The presence of blastema and the tendency for neo-filament formation were qualitatively corroborated. 18 gills were used for anatomical clearing and staining, 4 gills for microcomputed tomography (micro-CT).

Branchial arch selection

Taking into consideration that the first arch is widely exposed to environmental variations, our analysis was focused on the second left branchial arch. The first three arches share similarities in morphology, filament number, and regenerative patterns, although their relative length decreases progressively. These differences in size have not been associated with significant variations in regenerative processes. It is also important to highlight that in aquaculture practices and salmonid welfare assessments, the second arch is widely used as a standard reference for histological and morphological comparisons reinforcing the methodological validity of its selection (Bloecher et al., 2024; Clinton et al., 2024).

Anatomical clearing and staining

Samples destined for anatomical study were processed according to the clearing and staining protocol described by (Hanken and Wassersug, 1981). Specimens were stained with Alizarin Red-S to highlight the presence of calcium salts in ossified and calcified tissues. The protocol included immersion in 5% KOH for 24 h, followed by gradual transferring to 100% glycerin for preservation and visualization. The total number of gill filaments, as well as the number of calcified filaments were quantified.

Microcomputed tomography

Micro-CT analyses were performed with a BRUKER SkyScan 1278 system, kindly provided by the Faculty of Dentistry, University of Chile. The standard protocol was adapted to optimize the balance between resolution, scanning time, and image quality for gill tissue. The parameters used are listed below:

Data acquisition: Full 360° rotation of each sample.

Voltage: 40 kV Current: 215 μA

Camera pixel size: 9.0 µm; 2×2 binning, resulting in an effective

pixel size of 10 µm

Image reconstruction was performed with the NRecon v.1.6.9.18. software.

Ring artifact correction was applied in order to reduce visual interference, and the post-alignment adjustment was set at 18.50 to improve slice overlap accuracy.

Those adjustments yielded high-resolution images suitable for evaluating structural and morphological changes associated with gill regeneration.

Histological and morphological evaluation

From the 28 gills selected for light microscopy, $5 \mu m$ histological sections were obtained using a Microm microtome and mounted serially on glass slides. The histochemical techniques applied were: i) Alcian Blue, for mucus, mucus-secreting cells and hyaline cartilage matrix recognition; ii) Masson's Trichrome and Mallory's Trichrome, for connective tissue characterization.

Histopathological evaluation was conducted in all 28 fish gills considering: (1) branchial arch deformation, (2) epithelial hyperplasia, (3) lamellar fusion, (4) deformation of filament cartilage, and (5) cartilage calcification. A scoring system was applied in which the index 0 indicated normality and the indexes 2–5 reflected increasing degrees of morphological alterations. A subsample of 5 gills with scores close to 0–1 was selected, corresponding to individuals without arch deformities, cartilage alterations, or epithelial hyperplasia. This allowed us to ensure that morphometric and cellular quantifications were carried out on clinically normal fish specimens, minimizing the risk of bias from subclinical lesions.

Immunohistochemistry

Cell proliferation was evaluated using a mouse monoclonal anti-PCNA antibody (PC10, NeoBiotechnologies). Histological sections (5 μ m thickness) were obtained using a Microm HM315R microtome (Thermo Fisher Scientific, Waltham, MA, USA) and mounted on silanized slides.

Antigen retrieval was performed by 15 min incubation in a pressure cooker with antigen unmasking solution (Vector Laboratories, Newark, CA, USA). Blocking was obtained by 5 min incubation in PBS + BSA at room temperature. The tissues were incubated overnight at 4 °C, in the primary antibody diluted 1:200 in PBS. The secondary incubation in the conjugated polymer was performed at room temperature for 25 minutes. Diaminobenzidine (Vector Laboratories) was used as revelation agent.

Negative controls were obtained performing the complete protocol, omitting the primary antibody incubation step.

The monoclonal anti-PCNA antibody was chosen because it provided more reliable immunostaining in salmonids compared with Ki67.

For the calculation of the proliferation index, 50 nuclei were counted in randomly selected fields within the central cartilage zone of each filament. Among these, the number of nuclei showing positive immunoreactivity for PCNA was recorded. The proliferation index was expressed as the percentage of positive nuclei relative to the total nuclei counted (50), yielding values for 14 different filaments.

Morphometric measurements and statistical approach

Selected samples were scanned and digitized using a NanoZoomer XR C12000 microscope (Hamamatsu Photonics, Japan), generating Whole Slide Images (WSI). Quantifications were performed using the NDP.view2 software (Hamamatsu).

Quantitative measurements were extracted from digitized histological sections and analyzed using GraphPad Prism version 10 (Dotmatics, San Diego, USA). The data set considered paired measurements for each specimen and included the following parameters:

- i. Total gill area and blastema area (mm²).
- ii. Filament counts, subdivided in (a) Ft = total filaments per arch; (b) Fh = healthy filaments not associated with regeneration; (c) Fb = neo-filaments emerging from blastema.
- iii. Lamellar density, expressed as lamellae per filament per 0.5 mm² in healthy filaments and in filaments from the blastema zone.
- iv. Epithelial cell densities, quantified as mucus-secreting cells and ionocytes per 0.025 mm².
- v. Morphometric quantification was performed on n = 5 samples, following the protocol described by Mandarimde-Lacerda and del Sol (2017), who recommend including at least five cases per group as a sufficient sample size for statistically meaningful results.

Statistical analysis

Data was analyzed with the software GraphPad Prism 10 (GraphPad Software, Boston, Massachusetts USA). Results are

presented as mean \pm standard deviation (SD). All variables were treated as non-parametric based on Shapiro–Wilk tests. Wilcoxon signed-rank test was used to assess significant differences in lamellae per filament (0.5 mm²) and in cell densities (mucus-secreting cells and ionocytes per 0.025 mm²) within filaments. Correlations between variables were assessed with Spearman's test, considering a) Blastema area/number of neo-filaments; b) Blastema area/ionocytes and c) Blastema area/mucus-secreting cells.

The significance level was set at p < 0.05.

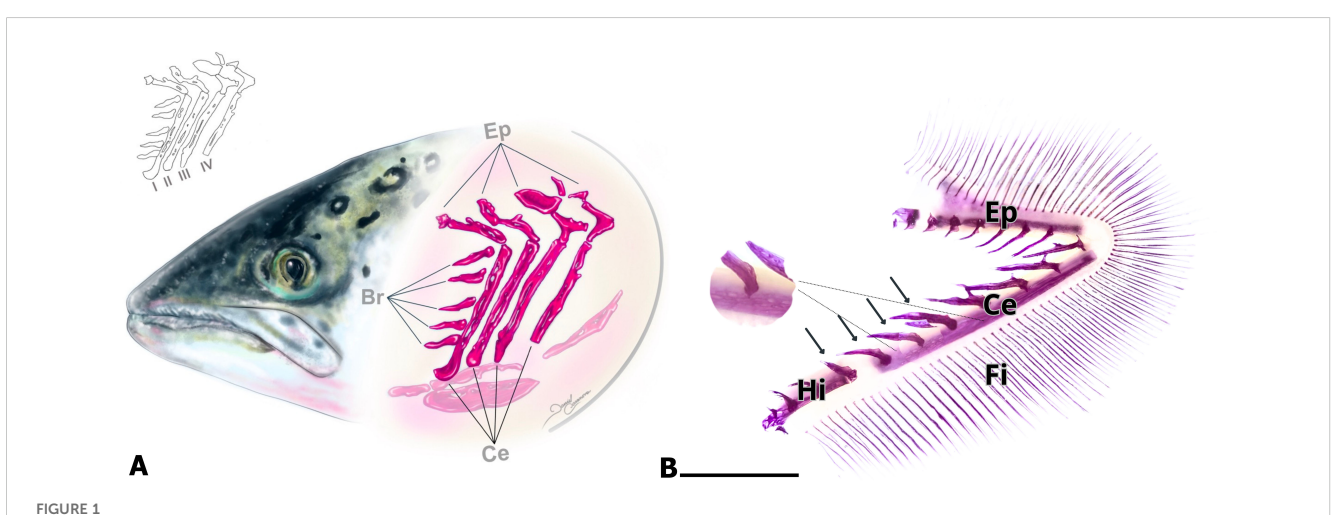
Results

Macroscopic analysis of the branchial arches and filaments

For a better understanding of the results, a diagram illustrating the shape and arrangement of the branchial arches has been included. Each arch is composed of the ceratobranchial (Ce), epibranchial (Ep), and hypobranchial (Hi) bones (Figure 1A), joined by a hyaline cartilage joint. The four ceratobranchial bones (I–IV) extend ventrally and display a relatively similar morphology. In contrast, the epibranchial bones, which project dorsally, are shorter and more irregular than those of the first arch (Figure 1A).

Anatomical techniques

The second gill arches of 18 fish were selected, diaphanized and stained with Alizarin Red to visualize the calcified tissues (Figure 1B). All gill bones and filaments appeared calcified, with mineralization extending through the basal two-thirds of the gills. Filaments were individually distinguished, arranged separately.



Atlantic salmon branchial arch. (A) Schematic representation of the arrangement of the four branchial arches. Each branchial arch (1, 2, 3, and 4) consists of three bones: epibranchial (Ep), ceratobranchial (Ce), and hypobranchial (Hi). The Ce bone has calcified branchial spines on the lateral side of its cortical region, and cavities are present in the bone matrix (shown in B). (B) Calcification of salmon gills in the freshwater phase. The ceratobranchial (Ce), epibranchial (Ep), and hypobranchial (Hi) bones, as well as the ossified and calcified branchial spines (arrows), are clearly observed. In its latero-lateral view, the cortical zone of the ceratobranchial bone is not compact. The presence of cavities indicates that it corresponds to porous bone. Calcified filaments (Fi) are also observed. Histological diaphanization and staining with alizarin. Calibration bar: 5 mm.

Micro-CT analysis

This analysis allowed detailed visualization of the bone structure of the branchial arches (Figure 2A), evidence that they are tubular in shape, presenting large pores and cavities on the lateral cortical surface (Figures 2A, B). Bone trabeculae and pores were also evident within the structure (Figure 2C). Similar features were observed in images obtained from the medial-lateral surface.

Microscopic analysis of the branchial arches

A total of 28 gills from freshwater smolt specimens were evaluated using light microscopy. The Ce and Ep bones displayed a tubular structure, with adipose tissue and bone trabeculae observed within them. Both branchial filaments and spines connected to the gill arches were clearly visible (Figure 3). Each filament contained a central axis of hyaline cartilage that extended toward the apical region, with lateral projections corresponding to the lamellae (Figures 2, 4A). The branchial filament epithelium was

composed of multiple cell types, including squamous cells, pillar cells, ionocytes and mucus-secreting cells (Figure 4).

Quantitative analysis of the branchial epithelium

All statistical values obtained are shown in Figures 5 and 6. Data showed a mean density of 8.88 ± 2.03 ionocytes per 0.025 mm² and 5.76 ± 0.91 mucus-secreting cells per 0.025 mm² (Figure 5). A Wilcoxon test revealed a significant difference between the two cell populations (p = 0.002), confirming that ionocytes are more abundant than mucus-secreting cells (Figure 4B).

Mechanisms of branchial regeneration

The histological analysis revealed that the gill regeneration zone is constituted by blastemal tissue, from which new filaments are generated (Figure 7A). We observed the formation of a regenerative blastema that initially gave rise to *de novo* filaments with developing lamellae. Subsequently, from the same blastema, a second

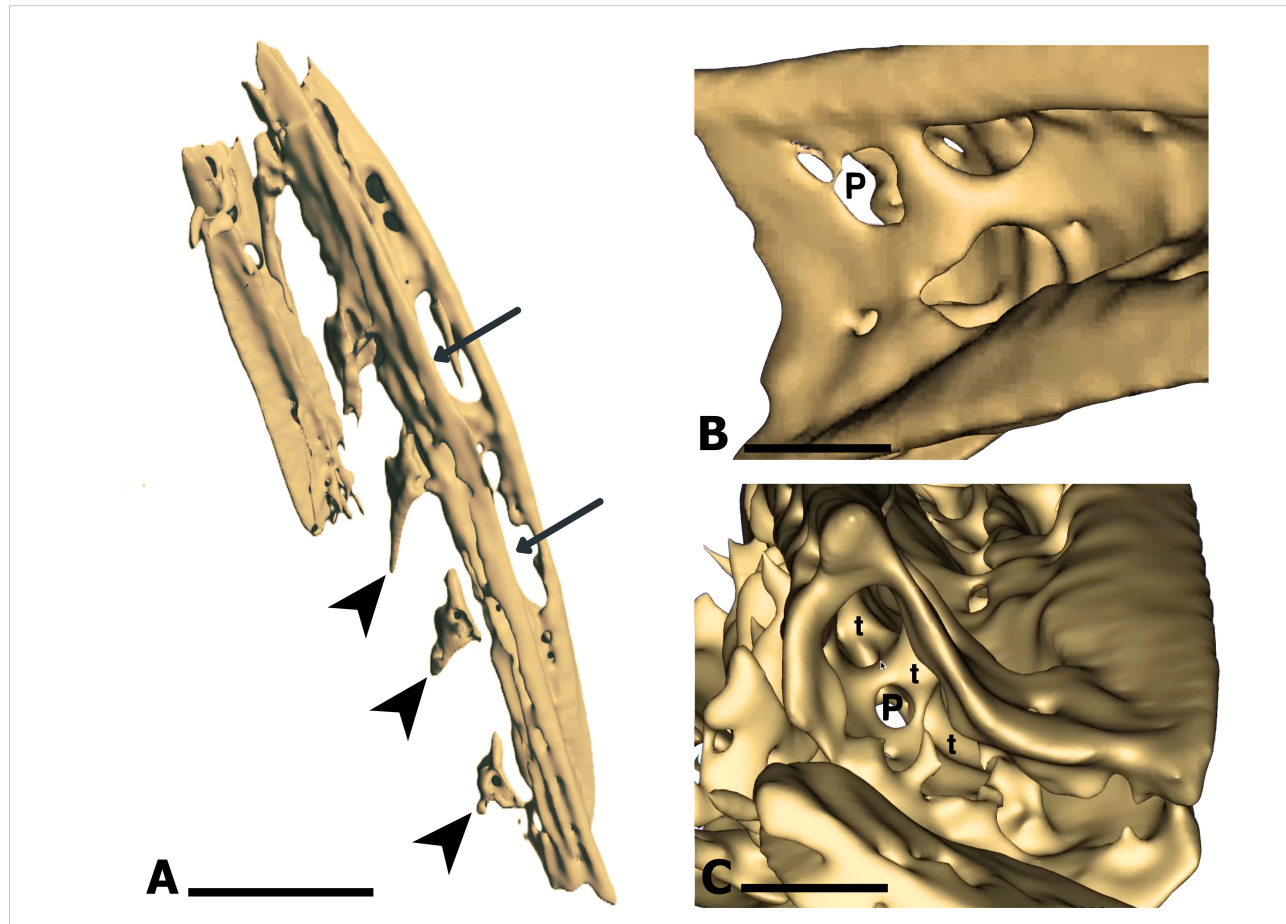


FIGURE 2

Tridimensional MicroCT reconstruction of the ceratobranchial (Ce) bone. (A) Lateral view of the Ce bone, showing cavities (arrows) on the external side, indicating a porous bone matrix. Dorsally located branchial spines (arrowhead) are also visible. (B) Detailed view of the external lateral surface of the Ce bone, highlighting large pores (P) that reflect a porous calcified matrix. (C) Internal view of the Ce bone, revealing the formation of trabeculae (t). Calibration bar: 5 mm (A), $250 \text{ } \mu \text{m}$ (B, C).

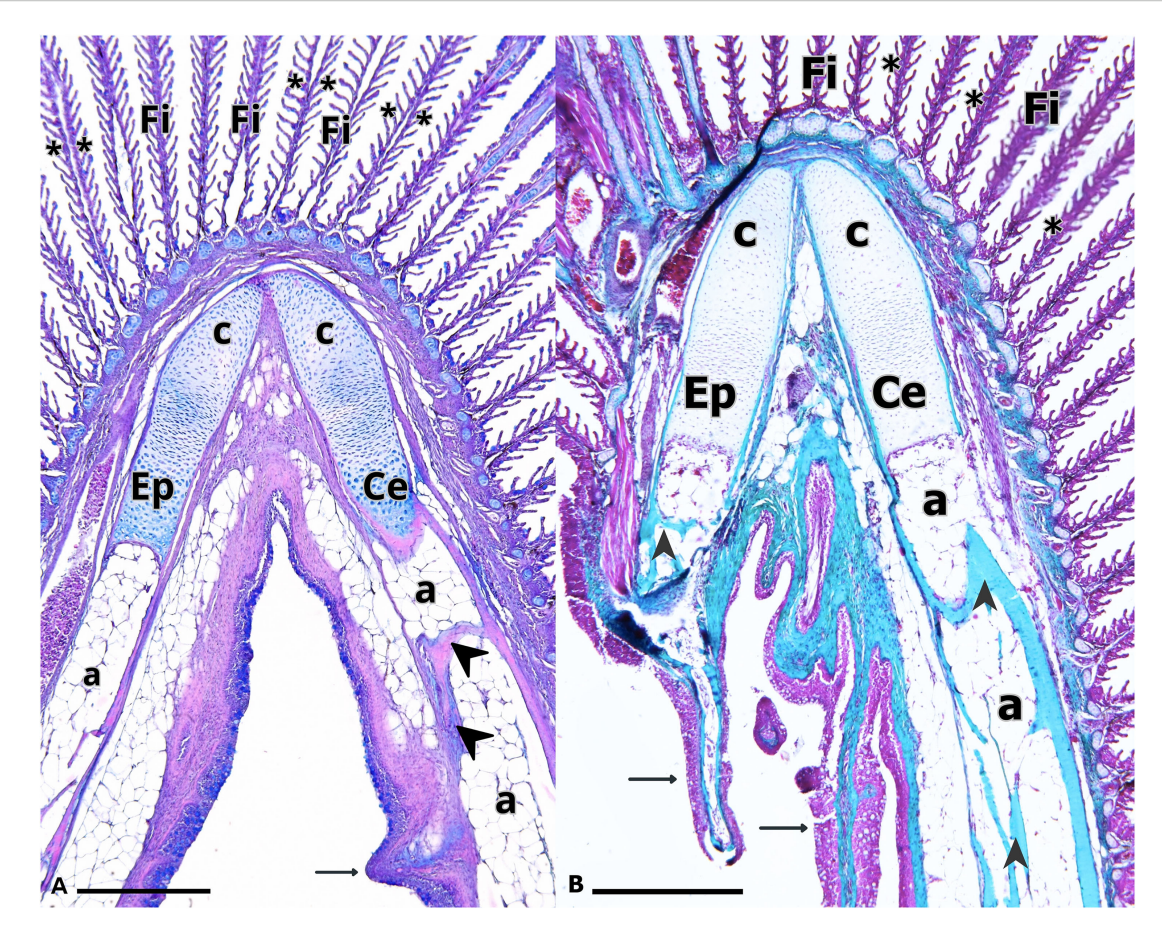


FIGURE 3
Branchial arch of Salmo salar. The Ceratobranchial and Epibranchial bones are connected by a joint of hyaline cartilage (c). Bone trabeculae (arrow heads) and adipose tissue (a) are observed. Branchial filaments (Fi), lamellae (asterisk) and branchial spines (arrows) are also observed. (A) H-E/Alcian blue and (B) Masson's Trichrome. Calibration bar: 2 mm.

generation of filaments emerged, indicating the capacity of this structure to produce multiple waves of filament outgrowth. The formation of a second generation of filaments involves the proliferation of blastema cells, leading to the initial development of lamellae (Figure 7B). Subsequently, differentiation occurs at the apices of the first-generation filaments, culminating in their connection with neighboring filaments (Figure 7C). Additionally, differentiation of the epithelial layer into mucus-secreting cells was observed.

Morphometric measurements showed that the total area occupied by branchial filaments was $68.32 \pm 10.1 \text{ mm}^2$, while the regeneration zone occupied $9.64 \pm 3.25 \text{ mm}^2$ (Figure 5). This indicates that in smolt salmon, the blastema represents between 8% and 19% of the total gill area, with an average of 14%.

The analysis of the filaments and their lamellae revealed marked differences between regions of the neo-filaments. In some areas, lamellae were entirely absent, while in others, lamellar neoformation was evident.

Microscopic observation revealed that the average number of filaments was 56.8 ± 3.1 . In non-regenerative zones, the mean was 20.4 ± 6.67 filaments, while regenerative zones had an average of 35.8 ± 8.81 filaments (Figure 5). A Wilcoxon test revealed a

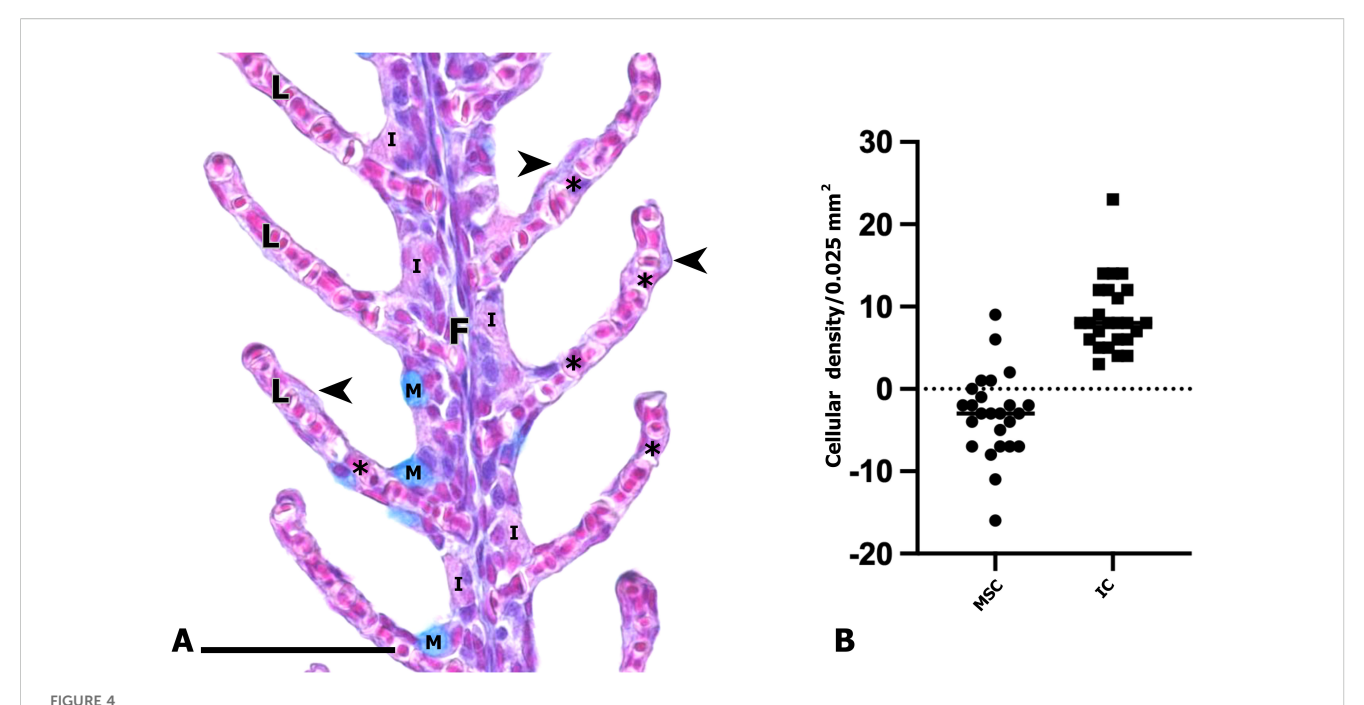
statistically significant difference between the two groups (p < 0.0001) (Figure 6A).

Within the blastema, the density of lamellae ranged from 0 to 55 (per $0.5~\text{mm}^2$). Lamellar density was lower in those filaments within the regenerating zone (33.84 \pm 15.86 per $0.5~\text{mm}^2$) compared to healthy filaments from the non-regenerating zones (48.56 \pm 19.34 per $0.5~\text{mm}^2$). This difference was significant (p = 0.0128), indicating incomplete lamellar development in regenerating structures (Figure 6B).

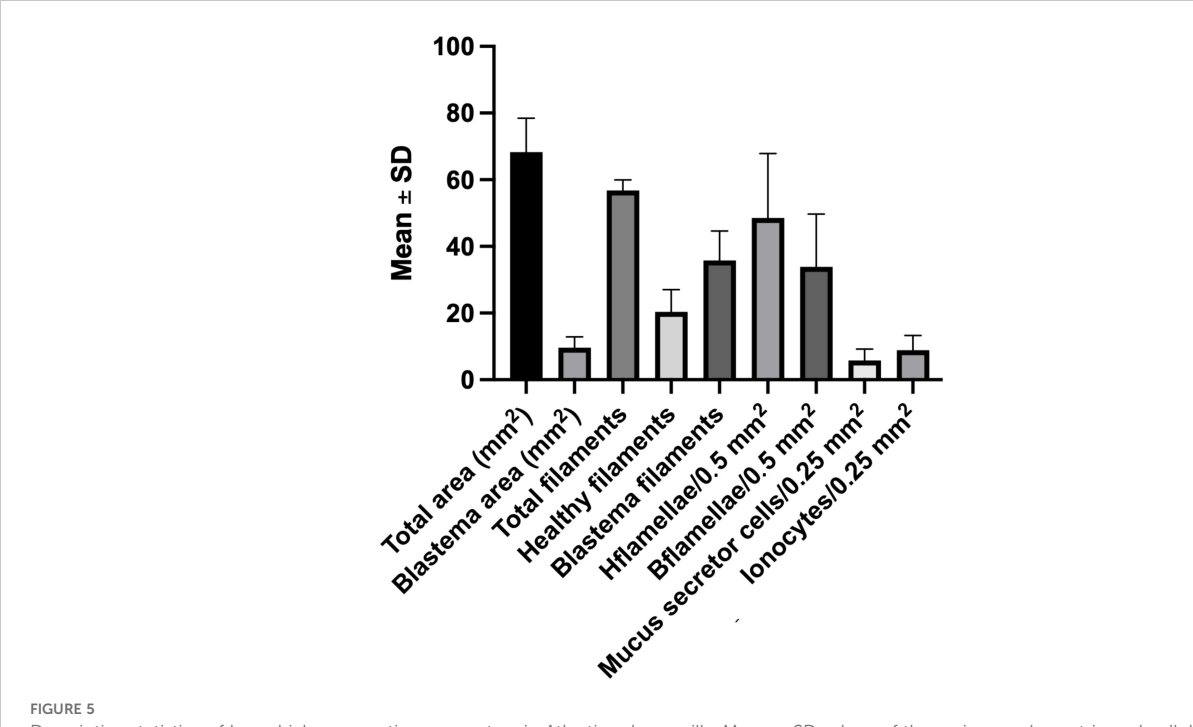
Correlation analysis (See Figure 6C) showed a positive association between the blastemal area and the number of regenerated filaments ($\rho = 0.5$, $p \approx 0.011$), supporting the role of blastemal tissue as the source of neo-filaments. These findings suggest that branchial regeneration is not necessarily accompanied by an immediate recovery of osmoregulatory capacity or epithelial protection during the phase of smoltification.

By contrast, no significant correlation was found between the blastemal area and lamella number ($\rho=0.206,\ p\approx0.323$) (Figure 6D). In a similar way, the correlation between ionocyte density and the blastemal area was not significant ($\rho=-0.03,\ p\approx0.888$) (Figure 6E), nor between mucus-secreting cells density and the blastema area ($\rho=-0.223;\ p\approx0.284$) (Figure 6F).

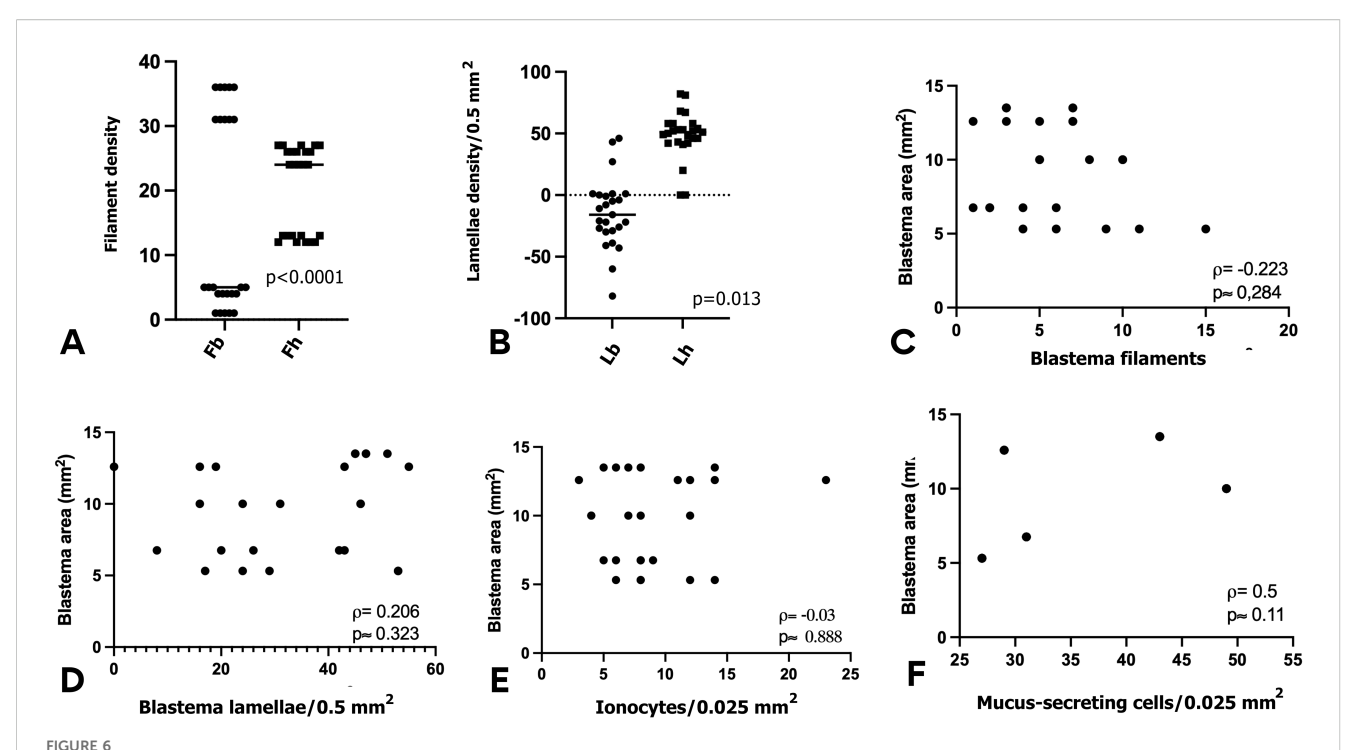
10.3389/fmars.2025.1682427 Smok et al.



(A) Branchial filament of Salmo salar. General view of a branchial filament showing lamellae (L) and various epithelial cell types, including pavement cells (arrowhead), pillar cells (asterisk), mucus-secreting cells (M), and ionocytes (I). Hematoxylin–Eosin/Alcian Blue staining. Scale bar: 50 µm. (B) Wilcoxon test comparing mucus-secreting cells and ionocytes densities (mucus cells /0.025 mm² vs. Ionocytes /0.025 mm²) revealed a significantly higher abundance of ionocytes (p < 0.01).



Descriptive statistics of branchial regenerative parameters in Atlantic salmon gills. Mean \pm SD values of the main morphometric and cellular variables quantified during gill regeneration. Parameters include: total area (At) and blastema area (Ab) (mm²), total filaments (Ft), healthy filaments (Fh), and blastema filaments (Fb); number lamellae per 0.5 mm² in healthy filaments (Lha) and in blastema filaments (Lb); densities of mucus-secreting cells (M) and ionocytes (I) per 0.025 mm²; and anatomical total filaments. Data represent pooled measurements across analyzed specimens and illustrate the variability underlying subsequent statistical comparisons. Error bars indicate standard deviations.



Statistical comparisons and correlations of gill regeneration parameters in Atlantic salmon smolts. (A, B) Wilcoxon signed-rank tests: (A) showed significant difference between number of blastema filament (Fb) and healthy filaments (Fh); (B) didn't show significance difference between lamellae density. (C-F) Spearman's rank correlations: showing positive correlation only between (C) Blastema area vs. regenerating filaments. Absence of correlation between blastema area and Blastema lamellae (D), ionocytes (E) and mucus secreting cells (F). All tests were performed in GraphPad Prism 10; p-values are indicated in each panel.

Tissue differentiation in the regeneration zone

It should be noted that the blastema corresponds to an undifferentiated tissue composed of proliferating cells with the potential to differentiate into various cell lines. In the present study, we observed that these cells give rise to sprouts that subsequently organize into *de novo* filaments with their respective lamellae. Furthermore, differentiation into striated muscle, smooth muscle associated with angiogenesis processes, and specialized connective tissues such as hyaline cartilage were also evident (Figure 8).

We also identified some areas that displayed two generations of filaments: the original ones formed during the fry stage, which were undergoing involution, and the neofilaments derived from the regenerating blastema (Figures 7 and 8). In some specimens, a second cohort of filament buds was also observed emerging from the same blastema (Figure 8A).

In the basal region of the blastema, an organized set of differentiating tissues was identified. Those tissues were arranged in an organized manner, making it possible to distinguish smooth muscle as well as the formation of blood vessels, which fuse basal to the epithelial buds, and increase their diameter to form each filament artery (Figure 8).

Smooth muscle differentiation was seen in the blastema, forming the wall of newly formed blood vessels (Figure 8). Underlying this layer, multinucleated muscle fibers with distinct transverse striations were differentiated. These striated muscle fibers

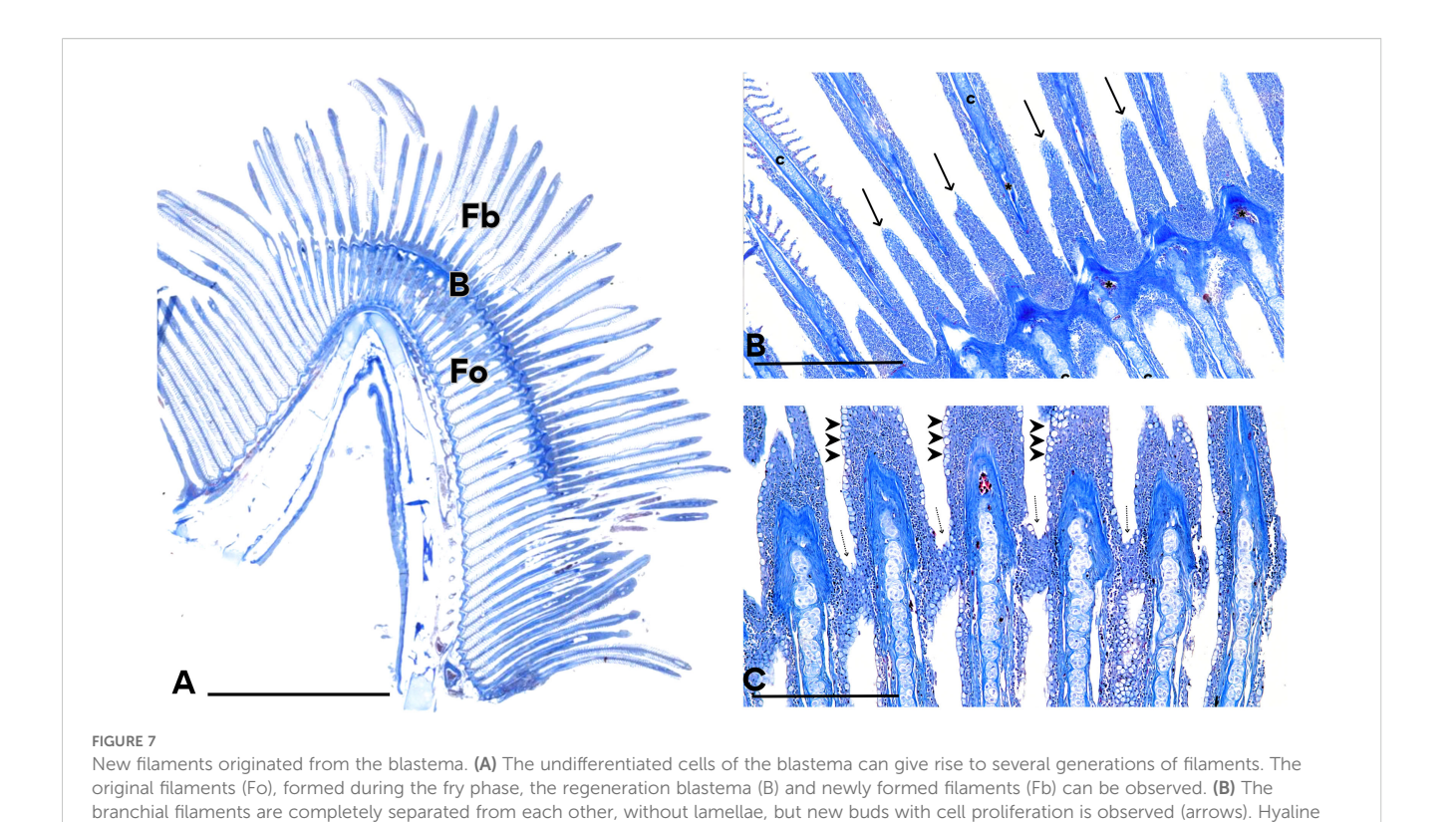
were arranged perpendicularly, extending from the blastema toward the base of the developing neofilaments (Figures 8).

Likewise, at the base of the neofilaments, the formation of hyaline cartilage was observed, projecting from the blastema towards the base and apical region of each filament. PCNA immunostaining revealed evident proliferative activity in the cartilage of branchial filaments (Figure 9A). The mean proliferation index was 38.9 \pm 13.5% (n = 14 filaments), with values ranging from 14% to 58% (Figure 9B). These findings confirm the presence of an actively dividing cell population within the filament cartilage, supporting its role as a primary substrate for filament regeneration.

Discussion

Gill plasticity and regenerative capacity

The branchial tissues of Atlantic salmon smolts display a remarkable plasticity and regenerative potential that provide the fish with the ability to adapt to environmental challenges, as it has been widely reported in teleosts (Chowdhury et al., 2022; Ghanizadeh-Kazerouni et al., 2024; Nilsson et al., 2012; Smok et al., 2025a, 2025b). The identification of histological patterns associated with adaptive remodeling—distinct from pathological lesions—provides valuable tools to refine diagnostic accuracy and to support monitoring of fish welfare in the aquaculture industry. Importantly,



cartilage (c) and blood vessels (asterisk) are also presented. C) Apical cells have proliferated and are arranged joining adjacent filaments (dotted arrow), forming a blastema of undifferentiated cells. Note the differentiation towards mucus-secreting cells (arrowhead). Mallory's Trichrome

these findings emphasize that not all cellular hyperplasia or filament remodeling should be interpreted as pathology but may represent some aspects of physiological regeneration.

Anatomy and functionality of branchial arches

staining. Calibration bars: 5 mm (A), 0.5 mm (B, C).

The ceratobranchial (Ce), epibranchial (Ep), and hypobranchial (Hi) bones of the branchial arches in smolt salmon correspond to unique tubular skeletal structures that present large pores or cavity. Traditionally, it has been postulated that tubular bones represent a functional adaptation to resist and absorb bending forces (Weigele and Franz-Odendaal, 2016). However, unlike previous descriptions, our analysis identified trabeculae and adipose tissue within these bones, suggesting additional resistance against deformation or fracture, attributable to their configuration as porous cortical bone.

A cartilage running along the entire filament provides structural rigidity that helps maintain filament orientation under continuous and sometimes turbulent water flow (Turko et al., 2020). Such a feature may represent an adaptive strategy to withstand mechanical stress in high-current environments or high-density aquaculture conditions (Smok et al., 2025a; Strzyzewska et al., 2016). By contrast, a proximal cartilaginous septum, as described in other salmonids, would allow greater distal flexibility (Thiruppathy et al., 2022). These differences may reflect an evolutionary trade-off between rigidity and respiratory efficiency.

Gill plasticity and remodeling capacity

We describe here that smolt salmon exhibits calcification not only in the branchial arches but also in all gill filaments and gill rakers. This result is consistent with previous studies in other fish species (Turko et al., 2020). However, it should be emphasized that this author did not describe calcification in salmon gill filaments. Calcification plays a crucial role in contributing to the structural firmness of filaments during respiratory cycles (Smok et al., 2025a). We observed that in *S. salar*, hyaline cartilage extends along the entire filament to the apex, conferring greater distal flexibility, in contrast to descriptions in other teleosts where it is restricted to the proximal region (Ghanizadeh-Kazerouni et al., 2024; Thiruppathy et al., 2022). This feature in salmon may reflect the need for greater rigidity to maintain filament orientation under continuous water flow.

Regenerative histology versus histopathology

It is of essential importance, for those laboratories that analyze salmonid gill health, to differentiate between regenerative histology and histopathological changes. Adaptive regeneration shows localized cellular hyperplasia at the filament tip until two or more filaments join followed by orderly differentiation into hyaline cartilage, smooth and striated muscle, mucus-secreting cells, and blood vessels. Our results are consistent with those reported by (Ghanizadeh-Kazerouni

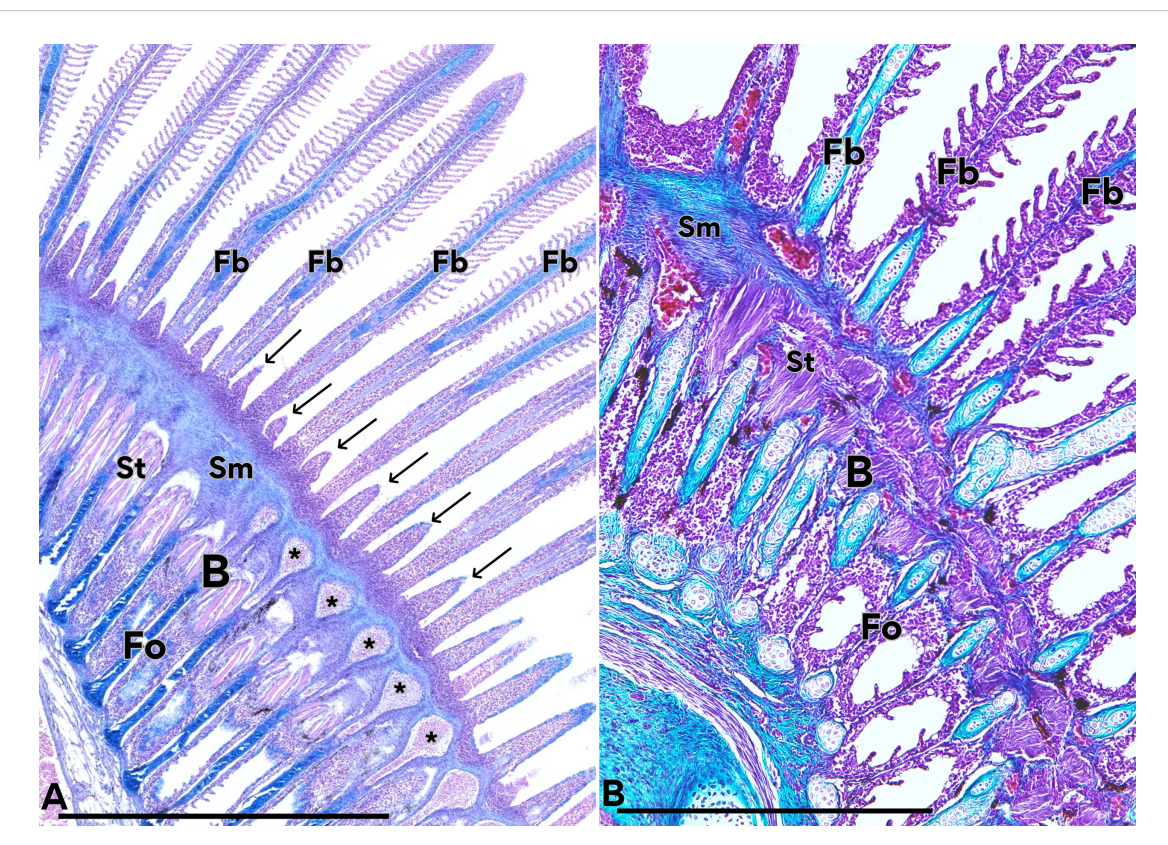
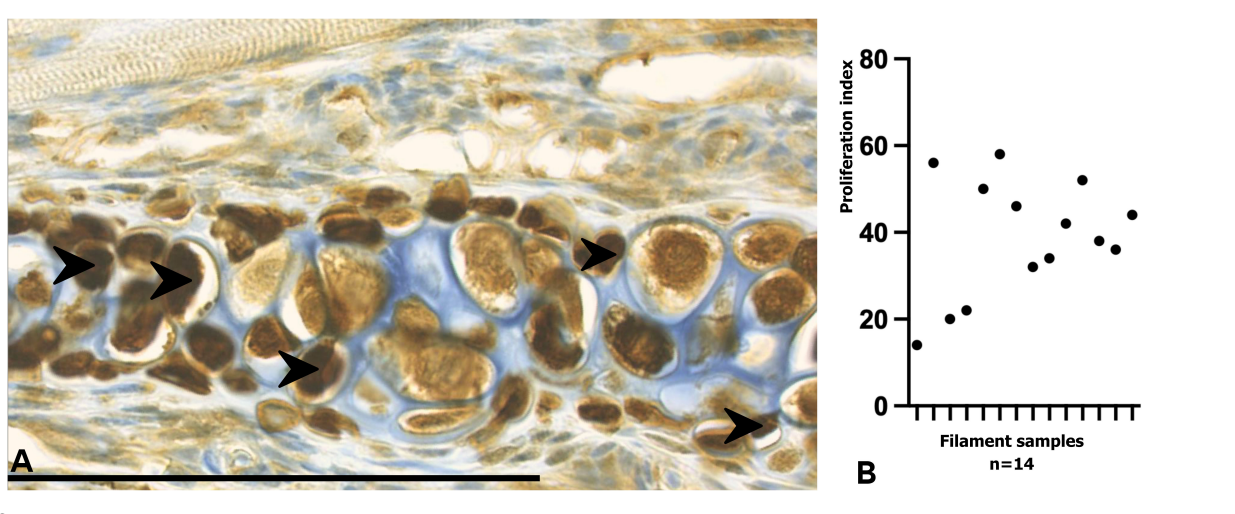


FIGURE 8
Tissues and structures originating from the regeneration zone. Regeneration blastema (B), original filaments (Fo) and neoformed filaments (Fb) are observed. Some cells of the blastema have differentiated into striated muscle tissue (St), which is distributed parallel to the filaments, while others have differentiated to smooth muscles (Sm) perpendicularly arranged and blood vessels (asterisk). A new generation of branchial buds is also observed (arrows). In B we can observe the first generation with cartilage inside it (Fb), and a second generation of undifferentiated cells emerging from the blastema (arrows). (A) Hematoxylin-Eosin/Alcian Blue, (B) Masson's trichrome. Calibration bars: 2 mm.



PCNA immunostaining and proliferation index of branchial filaments in *Salmo salar* smolts. (A) Immunohistochemical detection of PCNA in regenerating gill filaments. PCNA-positive nuclei (brown, arrows) were primarily localized within the hyaline cartilage of regenerating filaments, indicating active proliferative activity in this region. (B) Proliferation index of branchial filaments, showing an average value of approximately 39%, consistent with ongoing cell division during blastema-mediated regeneration. Each point represents the proliferation index measured for an individual filament. Calibration bar: 100 µm.

et al., 2024; Smok et al., 2025b, 2025a). In contrast, pathological processes display necrosis, inflammatory infiltration, diffuse disorganization, or neo-filaments lacking functional lamellae, which do not contribute to the respiratory process and reflect instead defective regeneration (Mitchell et al., 2012).

Filament regeneration without amputation

Previous studies have described blastema formation following gill amputation in fish (Jonz, 2024; Mierzwa et al., 2020). Our observations indicate that filament regeneration in Atlantic salmon can also occur without amputation, potentially triggered by environmental stressors such as hypoxia. In these cases, blastema formation occurred as bridges at the distal region of grouped filaments, generating a "second floor" of new filaments as the older ones regressed. This phenomenon resembles patterns reported by (Ghanizadeh-Kazerouni et al., 2024) and highlights a naturally occurring regenerative pathway distinct from those described in experimental models.

Blastema and filament regeneration

In smolt salmon, the blastema occupied an area that comprised between 8% and 19% of the total branchial area (mean \approx 14%) and correlated positively with the number of regenerated filaments, reinforcing its role as a proliferative hub. However, lamellar density was significantly lower in regenerating filaments, indicating incomplete lamellar development. These results suggest that filament regeneration does not immediately imply recovery of osmoregulatory or epithelial protection functions during smoltification, partially consistent with (Ghanizadeh-Kazerouni et al., 2024).

Branchial proliferation patterns detected with PCNA

Anti-PCNA immunostaining in our study showed active proliferation in filament cartilage, while epithelium and musculature were immune-negative tissues, consistent with what has been observed in already differentiated cells. PCNA index in filament cartilages reached a value of $39 \pm 4\%$. This complements the description of (Ghanizadeh-Kazerouni et al., 2024; Sales et al., 2017), who observed PCNA-immune-positive cells at the filament tips and in blastemas after resection in *S. salar*. The absence of an immune mark in epithelium and muscle, as observed in our study, likely reflects sampling at a later regenerative phase, in contrast to *Prochilodus lineatus*, a fish species where PCNA marks epithelial proliferation at early stages (Pastor et al., 2013).

Neo-filaments without lamellae as a transient stage

Our observations revealed neo-filaments without lamellae, mainly at the margins of the blastema and adjacent to nonregenerative areas. Similar structures have been described in zebrafish (*Danio rerio*) as epithelial extensions that may remain non-functional or later acquire distal lamellae, a process regulated by stem cell, niches at the filament tip (Mierzwa et al., 2020; Stolper et al., 2019). Comparative studies indicate that these early outgrowths act as reservoirs of undifferentiated cells with the capacity to generate functional respiratory units (Cadiz and Jonz, 2020). Thus, in Atlantic salmon, filaments lacking lamellae likely represent a transient stage of regeneration rather than a permanent defect, with their marginal localization minimizing respiratory impact while retaining the potential to differentiate under appropriate conditions.

Impact of environmental factors on gill regeneration

Several environmental and husbandry factors in commercial aquaculture may impose some limits to gill regeneration. Hypoxia, increased temperature, and environmental contamination affect blastema formation and differentiation, while high stocking densities increase the levels of stress and the susceptibility to infections. Altogether, these conditions promote defective regeneration—associated with neo-filaments without lamellae, disorganized hyperplasia, or inflammatory infiltration—in contrast to the adaptive patterns observed under controlled laboratory conditions (Jonz, 2024; Li et al., 2022; Liang et al., 2025).

Time required for filament regeneration

In laboratory model fish such as zebrafish and medaka, gill regeneration occurs relatively quickly, with replacement of most of the resected tissue within weeks or a few months (Jonz, 2024). In contrast, Atlantic salmon shows a much slower rate: by week 20, only an average of 38% of the amputated tissue had regenerated (Ghanizadeh-Kazerouni et al., 2024; Jonz, 2024; Mierzwa et al., 2020). Although salmon possess four pairs of branchial arches that provide some functional redundancy, a significant proportion of filaments undergoing regeneration present a reduced effective respiratory surface and may compromise seawater transfer. Therefore, assessing blastema extension and lamellar maturation could be a useful criterion to determine smolt readiness for transfer from freshwater to a marine environment.

Organization of striated musculature in gill regeneration

During regeneration, striated muscle fibers differentiate and emerge *de novo* from the blastema, in association with Sonic Hedgehog (Shh) signaling, which has been previously linked to muscle regeneration and differentiation (Roy and Gatien, 2008; Smok et al., 2025b). These muscle fibers are located in the basal

region of the blastema and play a key role in providing mobility and structural support to newly formed gill filaments (Johnston, 2006; Johnston and Hall, 2004). Smooth muscle fibers at the base of the filaments and around the cartilaginous axis are closely associated with developing blood vessels.

Limitations of zebrafish as a model compared to salmonid

Compared to zebrafish, where gill regeneration occurs rapidly at higher temperatures, regeneration in Atlantic salmon is slower and more dependent on the fish metabolic state (Ghanizadeh-Kazerouni et al., 2025; Jonz, 2024; Mierzwa et al., 2020). Studies performed in amphibian provide further parallels, with blastema formation and conserved signaling pathways such as FGF, BMP, Shh, and Wnt regulating tissue restoration (Roy and Gatien, 2008). Although in the present study we did not perform molecular analyses, the presence of neovascularization, undifferentiated cell proliferation at filament tips, and de novo striated muscle differentiation strongly suggests the involvement of canonical pathways, including HIF-VEGF, Shh and FGF, which have been implicated in zebrafish and mammalian regeneration (Smok et al., 2025b; Rojas et al., 2016). This interpretation is further supported by our previous studies in *S*. salar, where hypoxia activated HIF-1α and promoted angiogenesis during spinal cord and caudal fin regeneration (Rojas et al., 2007, 2024a, 2024b; Sánchez et al., 2011), indicating that similar mechanisms may also contribute to branchial regeneration.

In the present study we did not measure HIF-1α in salmon gills. The proposed link between hypoxia and HIF activation is therefore presented as a mechanistic hypothesis, supported by (i) literature describing the association between hypoxia, HIF activation, and neovascularization, and (ii) our previous findings in other tissues of Salmo salar under hypoxic conditions. Specifically, we have documented that parr and smolt stages display regenerative capacity in the spinal cord and caudal fin in response to reduced oxygenation, with HIF-1α activation and angiogenesis playing a central role (Rojas et al., 2024a, 2024b). Based on this evidence, we hypothesize that branchial regeneration may likewise be modulated by HIF-dependent mechanisms under hypoxic conditions. As a future experimental approach, we propose the direct evaluation of blastema tissue for HIF-1α (IHC), HIF-2α, VEGF/VEGFR, and other molecular markers, which will allow a conclusive demonstration of the involvement of this pathway in gill regeneration.

Limitations of the study

This work provides a detailed histological characterization of branchial regeneration in Atlantic salmon smolts maintained under freshwater conditions, but several limitations must be acknowledged. First, the sample size used for morphometric and cellular analyses was limited, following stereological recommendations and in agreement with the criteria reported by Mandarim-de-Lacerda and Mariano del Sol. Second, although morphological features such as proliferative blastema organization, neovascularization, and de novo muscle fiber differentiation suggest the possible involvement of canonical signaling pathways (e.g., Shh, FGF, BMP, and HIF-VEGF), no molecular or transcriptomic analyses were performed in this study. Thus, the proposed mechanistic associations remain hypothetical and should be confirmed in future research. Unlike zebrafish laboratory models, no gill ablation was performed in the present study. Instead, freshwater Salmo salar individuals were analyzed across ontogenetic development-from alevin to smolt stages—where a regenerative blastema was naturally identified and characterized. Finally, although PCNA immunostaining confirmed proliferative activity, this marker does not distinguish specific cellular lineages, limiting the interpretation of differential contributions to blastema formation. Nevertheless, the histological organization allows a clear recognition of epithelial, connective, cartilaginous, striated, and smooth muscle lineages within the regenerating tissue.

Perspectives

Future studies should integrate molecular analyses (e.g., transcriptomics, *in situ* hybridization, lineage tracing) with histological evidence to clarify the signaling pathways governing blastema formation and tissue differentiation. Expanding sampling across developmental stages (alevin, parr, smolt, adult) and environmental contexts (freshwater vs. seawater, laboratory vs. intensive aquaculture) will provide a more comprehensive understanding of the branchial regeneration dynamics. Particular attention should be paid to how environmental stressors—such as hypoxia, temperature fluctuations, and algal blooms—modulate the balance between adaptive remodeling and pathological processes. Translating these insights into aquaculture may lead to the development of regenerative biomarkers (e.g., blastema size, lamellar maturation, proliferation index) as practical criteria for smolt readiness and welfare assessment.

Conclusions

Branchial regeneration in *S. salar* is mediated by a proliferative blastema capable of differentiating into cartilage, epithelium, smooth muscle, striated muscle, and blood vessels. These findings highlight the fact that branchial regeneration is a physiological, non-pathological process playing an adaptive role during smoltification. Recognizing these histological criteria will allow for more accurate diagnosis, preventing the misinterpretation of regeneration as disease. Ultimately, incorporating regeneration-based indicators into aquaculture health monitoring may improve fish welfare and optimize the transfer of smolts from fresh to seawater.

Data availability statement

The original contributions presented in the study are included in the article/supplementary material. Further inquiries can be directed to the corresponding authors.

Ethics statement

The animal study was approved by Faculty Ethics Committee in ACTA No. 14321 of Research Project No. 072/21 of Universidad de La Frontera. The study was conducted in accordance with the local legislation and institutional requirements.

Author contributions

CS: Writing – review & editing, Methodology, Writing – original draft, Investigation, Formal Analysis. MR: Methodology, Validation, Writing – review & editing, Supervision, Funding acquisition, Investigation. MA: Writing – review & editing, Validation. Md: Validation, Project administration, Supervision, Writing – review & editing, Funding acquisition.

Funding

The author(s) declare financial support was received for the research and/or publication of this article. This study was supported by the Doctoral Program in Morphological Sciences of the Universidad de La Frontera (UFRO, Chile), which covered publication costs, and by the Comparative Embryology Laboratory of the Universidad de Chile and the Morphogenetic Lab – Veterinary Laboratory of Fish Ontogeny (Santiago, Chile), which contributed to histological and histochemical preparations. The funding bodies had no role in study design,

data collection/analysis, or manuscript preparation. We also thank Plataforma Experimental Bio-CT, Faculty of Dentistry, Universidad de Chile (FONDEQUIP EQM150010) for performing Micro-CT analysis.

Conflict of interest

The authors declare that the research was conducted in the absence of any commercial or financial relationships that could be construed as a potential conflict of interest.

Generative AI statement

The author(s) declare that Generative AI was used in the creation of this manuscript. Generative AI tools were used solely to improve the grammar, clarity, and style of the text. No AI tools were employed for data analysis, figure generation, or for creating, altering, or interpreting any scientific content. All research, analyses, and conclusions are entirely the work of the authors.

Any alternative text (alt text) provided alongside figures in this article has been generated by Frontiers with the support of artificial intelligence and reasonable efforts have been made to ensure accuracy, including review by the authors wherever possible. If you identify any issues, please contact us.

Publisher's note

All claims expressed in this article are solely those of the authors and do not necessarily represent those of their affiliated organizations, or those of the publisher, the editors and the reviewers. Any product that may be evaluated in this article, or claim that may be made by its manufacturer, is not guaranteed or endorsed by the publisher.

References

Bloecher, N., Østevik, L., Floerl, O., Sivertsgård, R., Aas, M., Kvaestad, B., et al. (2024). Evaluation of novel PCR-based method to assess gill injuries in fish caused by the cnidarian Ectopleura larynx. *Aquaculture Int.* 32, 6649–6663. doi: 10.1007/s10499-024-01482-8

Cadiz, L., and Jonz, M. G. (2020). A comparative perspective on lung and gill regeneration. J. Exp. Biol. 223, jeb226076. doi: 10.1242/jeb.226076

Cadiz, L., Reed, M., Monis, S., Akimenko, M.-A., and Jonz, M. G. (2024). Identification of signalling pathways involved in gill regeneration in zebrafish. *J. Exp. Biol.* 227, jeb246290. doi: 10.1242/jeb.246290

Chowdhury, K., Lin, S., and Lai, S.-L. (2022). Comparative study in zebrafish and medaka unravels the mechanisms of tissue regeneration. *Front. Ecol. Evol.* 10. doi: 10.3389/fevo.2022.783818

Clinton, M., Wyness, A. J., Martin, S. A. M., Brierley, A. S., and Ferrier, D. E. K. (2024). Association of microbial community structure with gill disease in marine-stage farmed Atlantic salmon (Salmo salar); a yearlong study. *BMC Vet. Res.* 20, 340. doi: 10.1186/s12917-024-04125-5

Costelloe, E., Lorgen-Ritchie, M., Król, E., Noguera, P., Bickerdike, R., Tinsley, J., et al. (2025). Microbial and histopathological insights into gill health of Atlantic salmon

 $(Salmo\ salar)$ across Scottish aquaculture sites. Aquaculture 599, 742166. doi: 10.1016/j.aquaculture.2025.742166

Fridman, S., Tsairidou, S., Jayasuriya, N., Sobolewska, H., Hamilton, A., Lobos, C., et al. (2021). Assessment of marine gill disease in farmed atlantic salmon (Salmo salar) in Chile using a novel total gross gill scoring system: A case study. *Microorganisms* 9, 2605. doi: 10.3390/microorganisms9122605

Ghanizadeh-Kazerouni, E., Wilson, J. M., Jones, S. R. M., and Brauner, C. J. (2024). Characteristics of a gill resection – Regeneration model in freshwater laboratory-reared Atlantic salmon (Salmo salar). *Aquaculture* 579, 740210. doi: 10.1016/j.aquaculture.2023.740210

Ghanizadeh-Kazerouni, E., Yoo, D. J., Jones, S. R. M., and Brauner, C. J. (2025). Impacts of severity and region of gill tissue resection on regeneration in Atlantic salmon (*Salmo salar*). Comp. Biochem. Physiol. Part A: Mol. Integr. Physiol. 302, 111815. doi: 10.1016/j.cbpa.2025.111815

Gjessing, M. C., Steinum, T., Olsen, A. B., Lie, K. I., Tavornpanich, S., Colquhoun, D. J., et al. (2019). Histopathological investigation of complex gill disease in sea farmed Atlantic salmon. *PloS One* 14, e0222926. doi: 10.1371/journal.pone.0222926

Hanken,, and Wassersug, (1981). The visible skeleton. Funct. Photog. 16, 22-26, 44.

Houde, A. L. S., Günther, O. P., Strohm, J., Ming, T. J., Li, S., Kaukinen, K. H., et al. (2019). Discovery and validation of candidate smoltification gene expression biomarkers across multiple species and ecotypes of Pacific salmonids. *Conserv. Physiol.* 7, coz051. doi: 10.1093/conphys/coz051

Johnston, I. A. (2006). Environment and plasticity of myogenesis in teleost fish. J. Exp. Biol. 209, 2249–2264. doi: 10.1242/jeb.02153

Johnston, I., and Hall, T. (2004). Mechanisms of muscle development and responses to temperature change in fish larvae. *Am. Fisheries Soc. Symposium* 40, 85–116.

Jonz, M. G. (2024). Cell proliferation and regeneration in the gill. *J. Comp. Physiol. B* 194, 583–593, doi: 10.1007/s00360-024-01548-2

Khaw, H. L., Gjerde, B., Boison, S. A., Hjelle, E., and Difford, G. F. (2021). Quantitative genetics of smoltification status at the time of seawater transfer in Atlantic salmon (Salmo salar). *Front. Genet.* 12. doi: 10.3389/fgene.2021.696893

Król, E., Noguera, P., Shaw, S., Costelloe, E., Gajardo, K., Valdenegro, V., et al. (2020). Integration of transcriptome, gross morphology and histopathology in the gill of sea farmed Atlantic salmon (Salmo salar): lessons from multi-site sampling. *Front. Genet.* 11. doi: 10.3389/fgene.2020.00610

Li, X., Ling, C., Wang, Q., Feng, C., Luo, X., Sha, H., et al. (2022). Hypoxia stress induces tissue damage, immune defense, and oxygen transport change in gill of silver carp (Hypophthalmichthys molitrix): evaluation on hypoxia by using transcriptomics. *Front. Mar. Sci.* 9. doi: 10.3389/fmars.2022.900200

Liang, H., Mi, H., Wang, K., Ren, M., Zhang, L., Huang, D., et al. (2025). Enhancement of Hypoxia Tolerance of Gibel Carp (Carassius auratus gibelio) *via* a Ferroporphyrin-Rich Diet. *Antioxidants* 14, 738. doi: 10.3390/antiox14060738

Luzio, A., Monteiro, S. M., Fontaínhas-Fernandes, A. A., Pinto-Carnide, O., Matos, M., and Coimbra, A. M. (2013). Copper induced upregulation of apoptosis related genes in zebrafish (Danio rerio) gill. *Aquat. Toxicol.* 128-129, 183–189. doi: 10.1016/i.auautox.2012.12.018

Mandarim-de-Lacerda, C. A., and del Sol, M. (2017). Tips for studies with quantitative morphology (Morphometry and stereology). *Int. J. Morphol.* 35, 1482–1494. doi: 10.4067/S0717-95022017000401482

McCormick, S. D. (2012). Smolt physiology and endocrinology. *En Fish Physiol.* 32, 199–251). doi: 10.1016/B978-0-12-396951-4.00005-0

Messerli, M., Aaldijk, D., Haberthür, D., Röss, H., García-Poyatos, C., Sande-Melón, M., et al. (2020). Adaptation mechanism of the adult zebrafish respiratory organ to endurance training. *PloS One* 15, e0228333. doi: 10.1371/journal.pone.0228333

Mierzwa, A. S., Nguyen, F., Xue, M., and Jonz, M. G. (2020). Regeneration of the gill filaments and replacement of serotonergic neuroepithelial cells in adult zebrafish (Danio rerio). *Respir. Physiol. Neurobiol.* 274, 103366. doi: 10.1016/j.resp.2019.103366

Mitchell, S. O., Baxter, E. J., Holland, C., and Rodger, H. D. (2012). Development of a novel histopathological gill scoring protocol for assessment of gill health during a longitudinal study in marine-farmed Atlantic salmon (Salmo salar). *Aquaculture Int.* 20, 813–825. doi: 10.1007/s10499-012-9504-x

Mitchell, S. O., and Rodger, H. D. (2011). A review of infectious gill disease in marine salmonid fish. J. Fish Dis. 34, 411–432. doi: 10.1111/j.1365-2761.2011.01251.x

Morera, F. J., Castro-Guarda, M., Nualart, D., Espinosa, G., Muñoz, J. L., and Vargas-Chacoff, L. (2021). The biological basis of smoltification in Atlantic salmon. *Austral J. Vet. Sci.* 53, 73–82. doi: 10.4067/S0719-81322021000100073

Nilsson, G. E. (2007). Gill remodeling in fish – a new fashion or an ancient secret? J.~Exp.~Biol.~210, 2403-2409. doi: 10.1242/jeb.000281

Nilsson, G. E., Dymowska, A., and Stecyk, J. A. W. (2012). New insights into the plasticity of gill structure. *Respir. Physiol. Neurobiol.* 184, 214–222. doi: 10.1016/j.resp.2012.07.012

Pan, W., Scott, A. L., Nurse, C. A., and Jonz, M. G. (2021). Identification of oxygensensitive neuroepithelial cells through an endogenous reporter gene in larval and adult transgenic zebrafish. *Cell Tissue Res.* 384, 35–47. doi: 10.1007/s00441-020-03307-5

Pastor, R., Sbodio, O., Stella Maris, G., Rojas, E., and Espíndola, B. (2013) Estudio inmunohistoquímico de proliferación (PCNA) en branquias de Prochilodus lineatus de las cuencas del río Salado y Paraná. *Redvet.* 14, 1–11, España.

Peñailllo, P. (2011). Estudio morfológico de branquias de alevines Salmo salar sometidos a hipoxia (Chile: Universidad de Chile).

Powell, M., Reynolds, P., and Kristensen, T. (2015). Freshwater treatment of amoebic gill disease and sea-lice in seawater salmon production: Considerations of water chemistry and fish welfare in Norway. *Aquaculture*. 448, 18–28. doi: 10.1016/j.aquaculture.2015.05.027

Roa, I., Castro, R., and Rojas, M. (2011). Deformación de Branquias en Salmónidos: Análisis Macroscópico, Histológico, Ultraestructural y de Elementos. *Int. J. Morphol.* 29, 45–51. doi: 10.4067/S0717-95022011000100007

Robertson, L. S., and McCormick, S. D. (2012). Transcriptional profiling of the parrsmolt transformation in Atlantic salmon. *Comp. Biochem. Physiol. Part D Genomics Proteomics* 7, 351–360. doi: 10.1016/j.cbd.2012.07.003 Rojas, M., Hernández, H., Smok, C., Pellón, M., Sandoval, C., Salvatierra, R., et al. (2024a). Effect of hypoxia in the post-hatching development of the salmon (Salmo salar L.) spinal cord. *Front. Mar. Sci.* 11. doi: 10.3389/fmars.2024.1451254

Rojas, D. A., Perez-Munizaga, D. A., Centanin, L., Antonelli, M., Wappner, P., Allende, M. L., et al. (2007). Cloning of hif- 1α and hif- 2α and mRNA expression pattern during development in zebrafish. *Gene Expression Patterns* 7, 339–345. doi: 10.1016/j.modgep.2006.08.002

Rojas, M., Saint-Pierre, G., Hartley, R., Vásquez, B., Conei, D., and Del Sol, M. (2016). Immunolocalization of morphogen sonic hedgehog in salmon fry (Salmo salar). *Int. J. Morphol.* 34, 770–774. doi: 10.4067/S0717-95022016000200054

Rojas, M., Salvatierra, R., Smok, C., Sandoval, C., Souza-Mello, V., and Del Sol, M. (2024b). Effect of hypoxia on the post-hatching growth of the body of the fry and the caudal fin of the Atlantic Salmon (Salmo salar). *Front. Mar. Sci.* 11. doi: 10.3389/fmars.2024.1425671

Roy, S., and Gatien, S. (2008). Regeneration in axolotls: A model to aim for! Exp. Gerontol. 43, 968–973. doi: 10.1016/j.exger.2008.09.003

Saito, N., Nishimura, K., Makanae, A., and Satoh, A. (2019). Fgf- and Bmp-signaling regulate gill regeneration in Ambystoma mexicanum. *Dev. Biol.* 452, 104–113. doi: 10.1016/j.ydbio.2019.04.011

Sales, C. F., Santos, K. P. E. D., Rizzo, E., Ribeiro, R. I. M. D. A., Santos, H. B. D., and Thomé, R. G. (2017). Proliferation, survival and cell death in fish gills remodeling: From injury to recovery. Fish & Shellfish Immunology. 68, 10–18. doi: 10.1016/j.fsi.2017.07.001

Sánchez, R. C., Obregón, E. B., and Rauco, M. R. (2011). Hypoxia is like an ethiological factor in vertebral column deformity of salmon (Salmo salar). *Aquaculture* 316, 13–19. doi: 10.1016/j.aquaculture.2011.03.012

Singh, J., Kumari, U., Prakash, R., Maiti, P., Mittal, S., and Mittal, A. K. (2025). Alterations in the epidermis and mucus viscosity of the carp, Cirrhinus mrigala, experimentally infected with Edwardsiella tarda. *Microb. Pathogen.* 207, 107883. doi: 10.1016/j.micpath.2025.107883

Slattery, O., Dahle, M. K., Sundaram, A. Y. M., Nowak, B. F., Gjessing, M. C., and Solhaug, A. (2023). Functional and molecular characterization of the Atlantic salmon gill epithelium cell line ASG-10; a tool for *in vitro* gill research. *Front. Mol. Biosci.* 10. doi: 10.3389/fmolb.2023.1242879

Smok, C., Rojas, M., and Del Sol, M. (2025a). Calcificación de Filamentos Branquiales en Salmo salar: Perspectivas sobre Plasticidad y Función. *Int. J. Morphol.* 43, 244–249. doi: 10.4067/S0717-95022025000100244

Smok, C., Rojas, M., and Del Sol, M. (2025b). Morphogenesis of Striated Muscle: An Analysis of its Regeneration in Gill Filaments of Salmo salar. *Int. J. Morphol.* 43, 901–907. doi: 10.4067/S0717-95022025000300901

Solhaug, A., Olsvik, P. A., Siriyappagouder, P., Faller, R., and Kristensen, T. (2024). Gill epithelial cell line ASG-10 from Atlantic salmon as a new research tool for solving water quality challenges in aquaculture. *Toxicol. Vitro* 96, 105790. doi: 10.1016/i.tiv.2024.105790

Sollid, J., De Angelis, P., Gundersen, K., and Nilsson, G. E. (2003). Hypoxia induces adaptive and reversible gross morphological changes in crucian carp gills. *J. Exp. Biol.* 206, 3667–3673. doi: 10.1242/jeb.00594

Stefansson, S. O., Haugland, M., Björnsson, B. T., McCormick, S. D., Holm, M., Ebbesson, L. O. E., et al. (2012). Growth, osmoregulation and endocrine changes in wild Atlantic salmon smolts and post-smolts during marine migration. *Aquaculture* 362-363, 127–136. doi: 10.1016/j.aquaculture.2011.07.002

Stolper, J., Ambrosio, E. M., Danciu, D.-P., Buono, L., Elliott, D. A., Naruse, K., et al. (2019). Stem cell topography splits growth and homeostatic functions in the fish gill. *eLife* 8, e43747. doi: 10.7554/eLife.43747

Strzyzewska, E., Szarek, J., and Babinska, I. (2016). Morphologic evaluation of the gills as a tool in the diagnostics of pathological conditions in fish and pollution in the aquatic environment: A review. *Vet. Med.* 61, 123–132. doi: 10.17221/8763-VETMED

Suarez, M., Del Sol, M., and Rojas, M. (2021). La Relevancia Moral del Dolor de Animales de Experimentación y de Producción. *Int. J. Morphol.* 39, 1383–1390. doi: 10.4067/S0717-95022021000501383

Sundell, K. S., and Sundh, H. (2012). Intestinal fluid absorption in anadromous salmonids: Importance of tight junctions and aquaporins. *Front. Physiol.* 3. doi: 10.3389/fphys.2012.00388

Thiruppathy, M., Fabian, P., Gillis, J. A., and Crump, J. G. (2022). Gill developmental program in the teleost mandibular arch. *eLife*. 11, e78170. doi: 10.7554/eLife.78170

Turko, A. J., Cisternino, B., and Wright, P. A. (2020). Calcified gill filaments increase respiratory function in fishes. *Proc. R. Soc. B: Biol. Sci.* 287, 20192796. doi: 10.1098/rspb.2019.2796

Weigele, J., and Franz-Odendaal, T. A. (2016). Functional bone histology of zebrafish reveals two types of endochondral ossification, different types of osteoblast clusters and a new bone type. *J. Anat.* 229, 92–103. doi: 10.1111/joa.12480